Dalton Transactions

Accepted Manuscript

ROYAL SOCIETY OF CHEMISTRY

www.rsc.org/dalton

Dalton

RSCPublishing

ARTICLE

Argentivorous Molecules Bearing Three Aromatic Side Arms: Synthesis of Triple-Armed Cyclens and Their Complexing Property towards Ag^+

Cite this: DOI: 10.1039/x0xx00000x

Received 00th January 2012,
Accepted 00th January 2012

DOI: 10.1039/x0xx00000x

www.rsc.org/

Yoichi Habata,*[a,b] Juli Kizaki,[a] Yasuhiro Hosoi,[a] Mari Ikeda,[b,c] and Shunsuke Kuwahara[a,b]

Triple-armed cyclens bearing three aromatic side-arms were prepared via three steps from (3*R*,5*S*)-3,5-dimethyl-1,4,7,10-tetraazacyclododecane-2,6-dione, and the Ag^+-ion-induced ^1H NMR and UV-vis spectral changes and X-ray structures suggested that the aromatic side-arms cover the Ag^+ incorporated in the ligand cavities like an insectivorous plant (Venus flytrap).

Introduction

In the past decade, cyclen has been widely used as an ion recognition site in metal ions sensors, building block for supramolecular structures, catalytic drugs, chirality signaling, MRI and fluorescent probes for imaging and so on.[1] Recently, we have reported[2] that tetra-armed and double-armed cyclens with aromatic side-arms behave like an insectivorous plant (Venus flytrap) when they form complexes with Ag^+. The aromatic side-arms in the armed-cyclens cover the Ag^+ incorporated in the cyclen cavities by Ag^+–π and CH–π interactions in an organic solvent as well as in water. The diameter of the cavity of cyclen, which is a 12-membered ring, is small for Ag^+, and an Ag^+ ion incorporated in the cyclen unit is exposed on the surface of the cyclen ring to allow Ag^+–π interactions between the Ag^+ and the aromatic side-arms. This behavior is not observed in Ag^+ complexes with benzyl-armed diaza-18-crown-6 ethers,[3] because CH–π interactions between aromatic rings are no possible in the diaza-18-crown-6 ether derivatives. We named the armed cyclens an "argentivorous molecule."[4] The aromatic side-arms in tetra-armed cyclens cover the Ag^+ incorporated in the cyclen cavity, even though electron withdrawing groups such as F, NO_2, and COO^- groups are introduced to the phenyl rings, all four aromatic side-arms cover the Ag^+ in the tetra-armed cyclens. On the other hand, the double-armed cyclens bearing naphthalene, anthracene, and pyrene which have higher electron density than substituted benzenes cover the Ag^+, however, the double-armed cyclens bearing phenyl rings as side-arms do not cover the Ag^+.[2d] These results indicate that Ag^+–π interaction between the Ag^+ and aromatic side-arms as well as CH–π interactions between neighboring aromatic rings are important for the dynamic conformational changes in the armed-cyclens. In a continuation of our previous work, we prepared triple-armed cyclens in order to answer the following questions. (i) In triple-armed cyclens bearing three phenyl rings, whether the aromatic side-arms cover the Ag^+ or not. (ii) If the aromatic side-arms cover the Ag^+ in the triple-armed cyclens, when a combination of two kinds of aromatic rings are introduced into a cyclen as side-arms, whether the substituent effects on the phenyl groups can be observed or not. (iii) In the tetra-armed cyclens, some Ag^+ complexes were a mixture of Δ and Λ forms in the solid state as shown in Figure 1. The CH–π interactions in triple-armed cyclen/Ag^+ complexes may be weaker than those in tetra-armed cyclen/Ag^+ complexes because triple-armed cyclens lack one aromatic ring. Therefore, we expected that the inversion of the side-arms (Δ and Λ forms) would be observed. During research efforts on the study of tetra-armed cyclen with two chiral centers on the cyclen ring, we found that (3*R*,5*S*)-3,5-dimethyl-1,4,7,10-tetraazacyclododecane-2,6-dione (*meso*-**6**) affords triple-armed cyclens selectively. Here, we report the synthesis of triple-armed cyclens with two methyl groups, the structures of Ag^+ complexes in solution and in the solid-state, and the inversion barrier of the Δ and Λ forms.

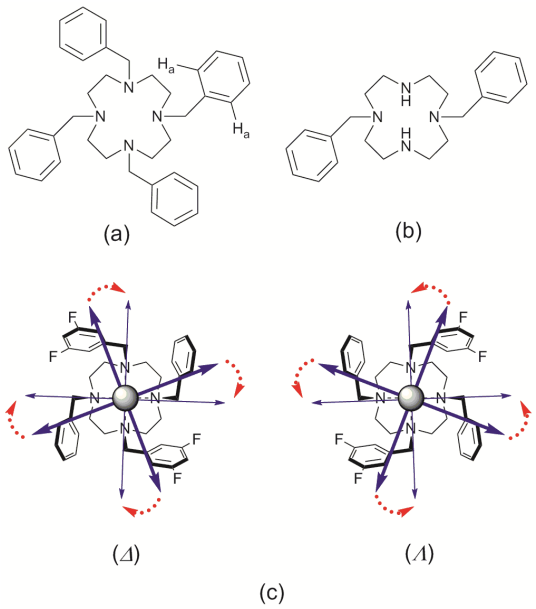

Figure 1. Tetra-armed (a) and double-armed (b) cyclens bearing benzenes as side-arms. Definition of the *Δ* and *Λ* forms in tetra-armed cyclens (c).

Results and discussion

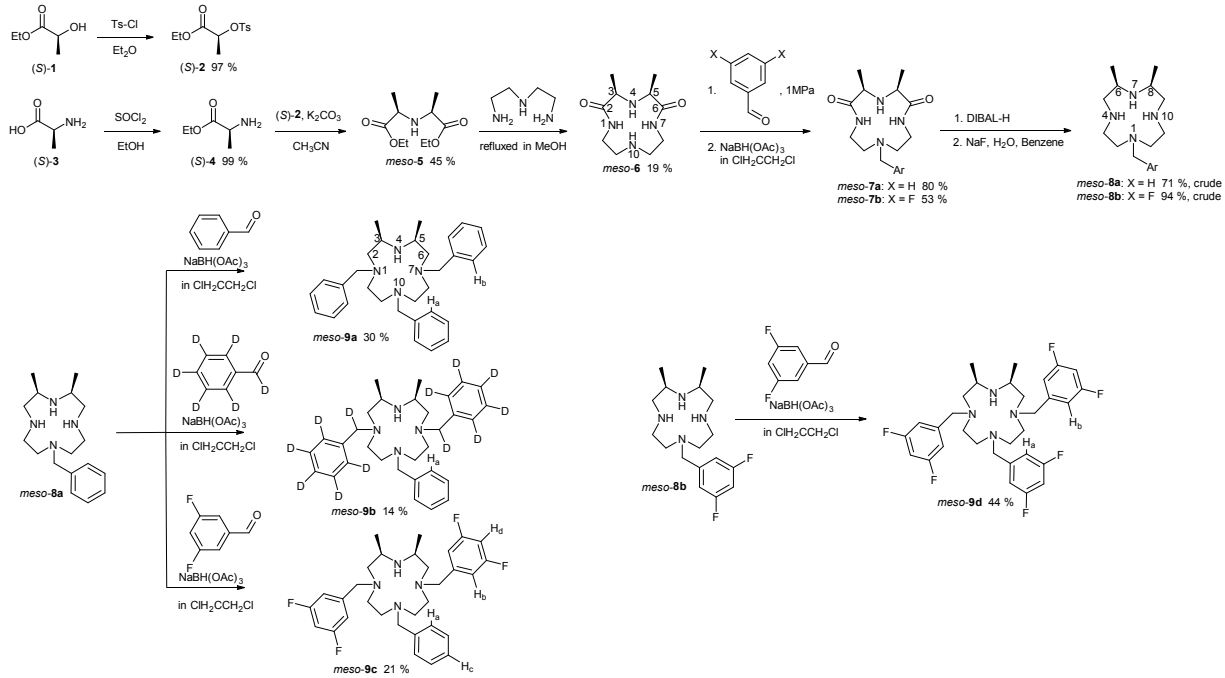

Scheme 1

Triple-armed cyclens were prepared as follows; (*S*)-(–)-Lactic acid tosylate ((*S*)-**2**)[5] and ethyl L-alaninate ((*S*)-**4**)[6] were prepared from (*S*)-(–)-lactic acid and L-alanine, respectively. (2*S*,2'*R*)-Diethyl 2,2'-iminodipropionate (*meso*-**5**)[7] was prepared by the reaction of (*S*)-**2** with (*S*)-**4** in the presence of K_2CO_3. Cyclization of *meso*-**5** with iminodiacetic acid affords (3*R*,5*S*)-3,5-dimethyl-1,4,7,10-tetraazacyclododecane-2,6-dione (*meso*-**6**). When reductive amination of *meso*-**6** was carried out using benzaldehyde and 3,5-difluorobenzaldehyde in the presence of $NaBH(OAc)_3$, 10-substituted derivatives (*meso*-**7a** and *meso*-**7b**) were obtained.

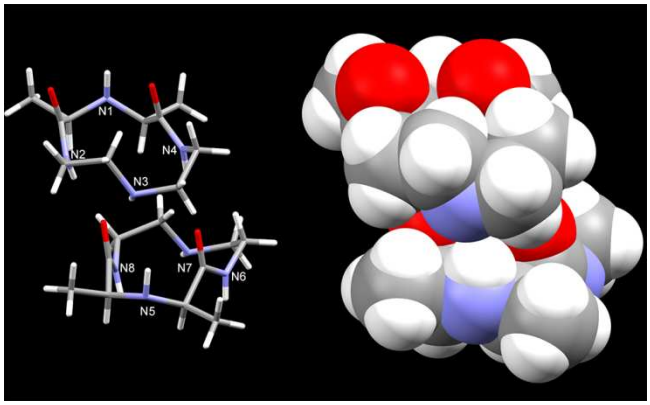

Figure 2. X-ray structure of *meso*-**6**. Steric hindrance by the two methyl groups inhibits the reductive amination at the 10-position nitrogen (N1 and N5).

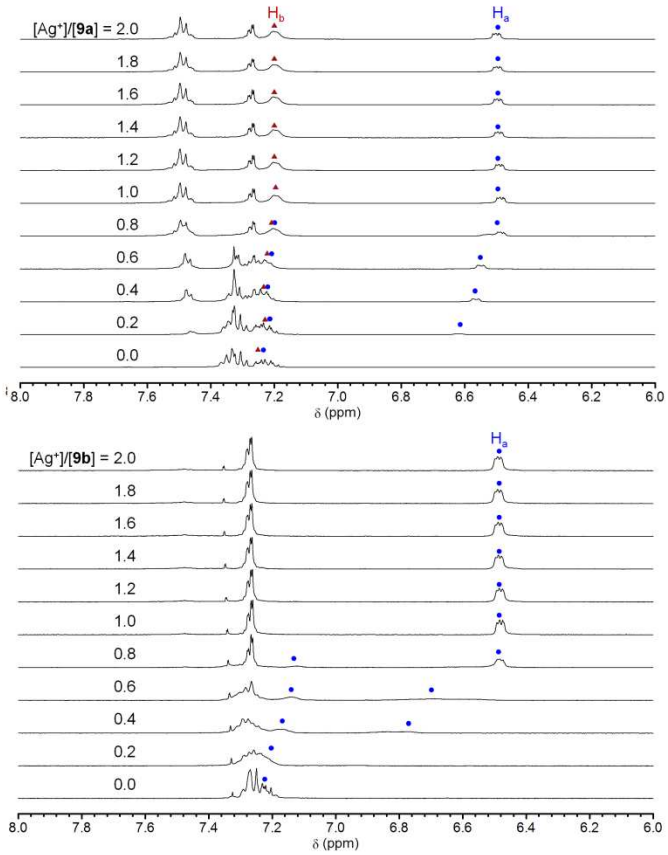

Figure 3. Ag^+-induced ^1H NMR spectral changes of *meso*-**9c** (top) and *meso*-**9d** (bottom) in CD_2Cl_2/CD_3OD.

The X-ray structure of *meso*-**6** (Figure 2) indicates that the N atom (at the 4-position in the cyclen) between the two methyl-substituted carbons does not react owing to the steric hindrance of the neighboring two methyl groups. Disubstituted compound, therefore, would not be obtained. After *meso*-**8a** and **8b** were obtained by the reduction of *meso*-**7a** and **7b**, the crude *meso*-**8a** and **8b** were used to reductive amination with benzaldehyde derivatives. Finally triple-armed cyclens (*meso*-**9a**–*meso*-**9d**) were obtained.

Structure of an Ag^+ complex with *meso*-**9a** was examined by Ag^+-induced ^1H NMR chemical shift changes (Figure 3). To assign the protons at the 2'- and 6'-positions in each aromatic rings, COSY, HMBC, and HMQC of a 1:1 (= *meso*-**9a** : Ag^+) mixture were measured (See Figures S9–S12b in the Electric Supplementary information (ESI)). In addition, an analogue of *meso*-**9a** (*meso*-**9b**) bearing deuterated benzenes at the 1- and 7-positions was also prepared to clarify the chemical shift of the phenyl protons at the 10-position. As shown in Figure 3, the aromatic H_a protons at the 10-position in the cyclen ring shifted to higher field ca by 0.74 ppm while the aromatic H_b protons at the 1- and 7-positions shifted to higher field ca by 0.13 ppm.

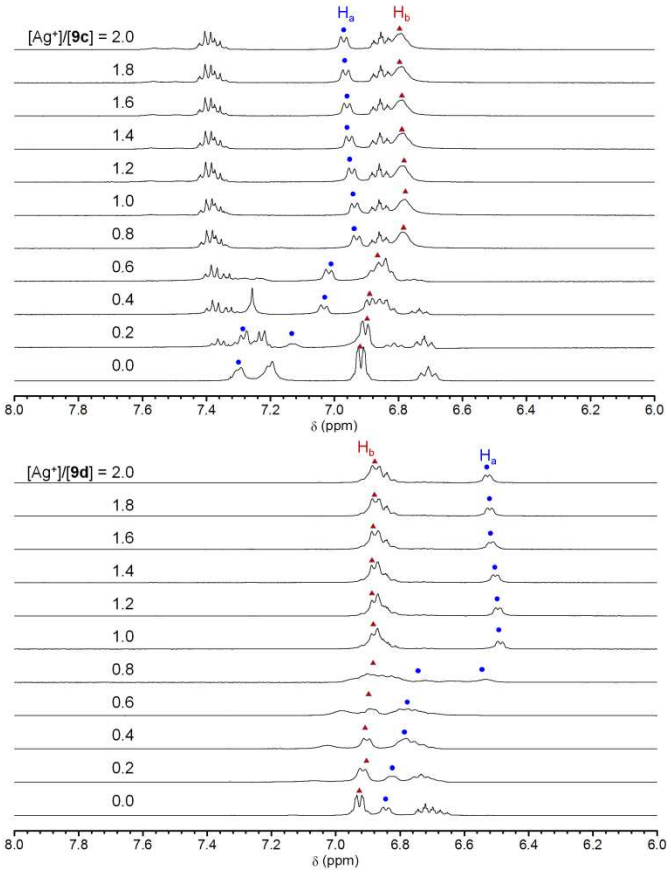

Figure 4. Ag^+-induced ^1H NMR spectral changes of *meso*-**9c** (top) and *meso*-**9d** (bottom) in CD_2Cl_2/CD_3OD.

On the other hand, the H_a protons in *meso*-**9c** and *meso*-**9d** which have 3,5-difluorobenzenes at the 1- and 7-positions in the cyclen, shifted to higher field ca by 0.36 ppm (Figure 4). The H_b protons in *meso*-**9c** shifted to higher field ca by 0.13 ppm. The value is similar with the H_b protons in *meso*-**9a**.

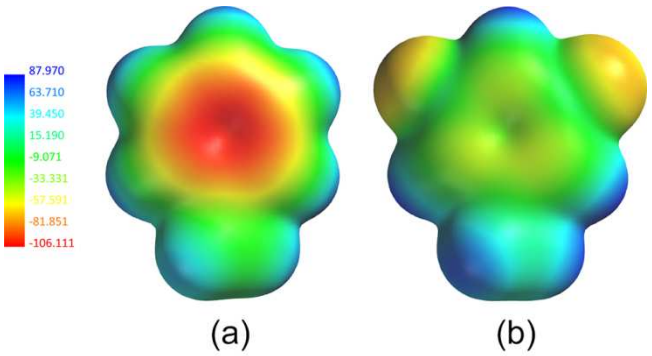

Figure 5. Electrostatic potential maps of (a) toluene and (b) 1,3-difluoro-4-methylbenzene (Property range: kJ/mol).

Figure 5 shows electrostatic potential maps, calculated using the B3LYP/6-31G(*) method,[8] of the toluene and 1,3-difluoro-4-methylbenzen. The electrostatic potential maps show that the electron densities in toluene is higher than that in 1,3-difluoro-4-methylbenzene. These chemical shift changes strongly support that the chemical shift changes of the H_a and H_b protons are affected by the electron density on the next aromatic rings. These chemical shift changes are summarized in Table 1.

Table 1. Ag^+-induced-^1H NMR chemical shift changes (Δppm)

Compd.	H_a (10-position)	H_b (1- and 7-positions)
meso-**9a**	–0.7	–0.13
meso-**9b**	–0.74	—
meso-**9c**	–0.36	–0.13
meso-**9d**	–0.36	–0.04

Negative values mean higher field shift.

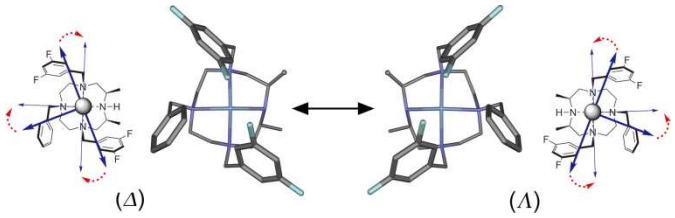

Figure 6. Optimized structures of *Δ* and *Λ* enantiomers of *meso*-**9b**/Ag^+ complex (B3LYP/6-31G*). Hydrogen atoms are omitted to clarify.

As we previously reported,[2c,2d] the aromatic protons at the 2'- and 6'-positions of aromatic side-arms (the H_a protons in Figure 1) in the tetra-armed cyclen bearing four phenyl groups shifted to higher field ca by 0.96 ppm. The higher field shift changes in the triple-armed cyclens indicate that the aromatic side-arms of *meso*-**9a**–**9d** cover the Ag^+ incorporated in the cyclen cavities. Small chemical shift changes of H_b protons at the 1- and 7-positions would be due to the absence of an aromatic side-arm at the 4-position nitrogen and rapid inversion between *Δ* and *Λ* enantiomers (Figure 6). It is important to note that symbols *Δ* and *Λ* refer to the helicity of the pendant arms.

To estimate the inversion barrier between *Δ* and *Λ* forms of *meso*-**9b**, VT ^{1}HNMR experiments of a 1:1 mixture of *meso*-**9b** and Ag^+ in CD_2Cl_2/CD_3OD were carried out in the range of 293 K–193 K (Figure 7).

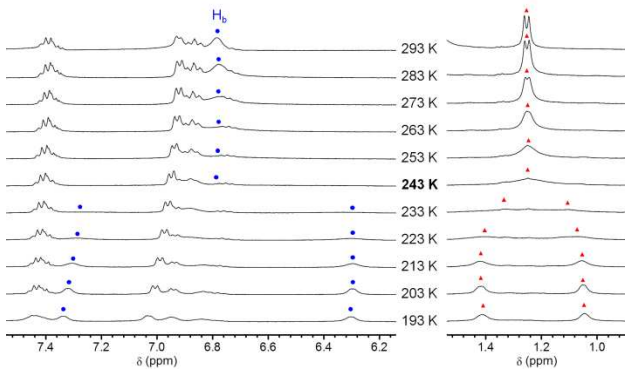

Figure 7. VT ^{1}H NMR experiments of *meso*-**9b**/Ag^+ in CD_2Cl_2/CD_3OD.

As shown in Figure 7, the coalescence temperature was observed at 243 K for the H_b protons in the phenyl rings at the 1- and 7-positions and the methyl protons. The inversion barrier ($\Delta G^{\ddagger}$) was estimated to be 11 kcal/mol using the methodology previously described by Shanan-Atidi and Bar-Eli.[9] This is the first example of inversion barrier in Ag^+ complexes with double-, triple-, and tetra-armed cyclens.

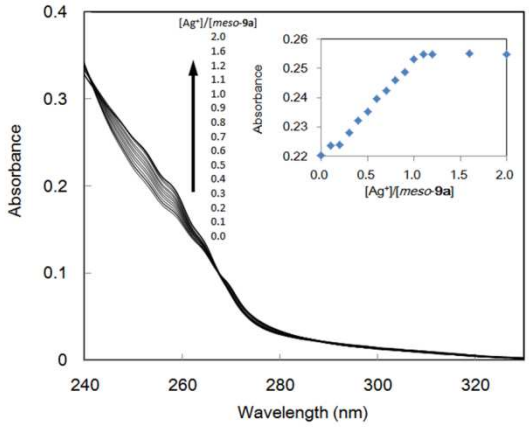

Figure 8. Ag^+-induced-UV-vis spectral changes of *meso*-**9a**/Ag^+ in CH_3CN.

Titration experiments using UV spectra were carried out to confirm the Ag^+–π interactions in CH_3CN. Figure 7 shows the Ag^+-ion-induced UV spectral changes of *meso*-**9a** (and Figures S25 and S26 in the ESI for *meso*-**9c** and *meso*-**9d**, respectively). An increase in the absorbance between 242 and 267 nm was observed with isosbestic points at 242 and 267 nm, upon the addition of Ag^+. An inflection point was observed at 1.0 (= $[Ag^+]/[meso\text{-}\mathbf{9a}]$), showing a 1:1 complex. Nonlinear least-squares analyses of the titration profiles clearly indicated the formation of 1:1 complex, and allowed us to estimate the association constants defined as eqn (1). The log*K* values between the ligands (*meso*-**9a**, *meso*-**9c** and *meso*-**9d**) and Ag^+ in CH_3CN were estimated to be ca. 5.6, 6.5, and 6.5, respectively, using HYPERSPC calculation program.[10]

$$\textbf{Ligand} + Ag^+ \rightleftharpoons [\textbf{Ligand}\text{–}Ag^+] \qquad (1)$$

K = [**Ligand**–Ag^+]/[**Ligand**][Ag^+]

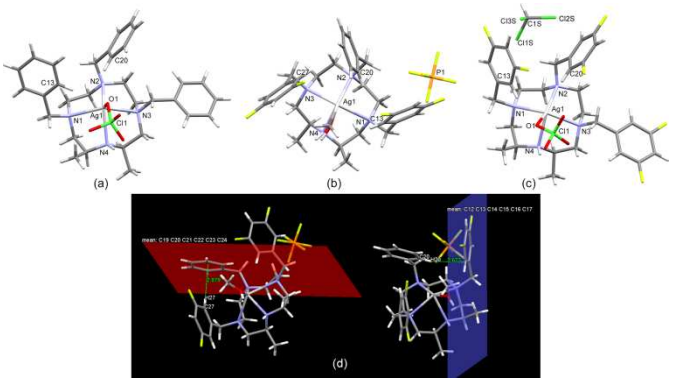

Figure 9. X-ray structures of (a) *meso*-**9a**/$AgClO_4$, (b) *meso*-**9c**/$AgPF_6$, (c) *meso*-**9d**/$AgClO_4$, and (d) C-H–plane distances of *meso*-**9c**/$AgPF_6$.

X-ray structures of Ag^+ complexes with the triple-armed cyclens were measured (Figure 9). In *meso*-**9b**/$AgPF_6$, three side-arms cover the Ag^+ and the C13–Ag1, C20–Ag1, and C27–Ag1 distances are 3.709, 3.179, and 3.613 Å, respectively. We reported that typical C–Ag distances range in tetra-armed cyclens is 3.272–3.344 Å[2b, 2d], and the 3.6–3.7 Å is relative long distances. These longer distances would be due to the absence of an aromatic side-arm at the 4-position nitrogen. In addition, intramolecular CH–π interactions between the aromatic rings are also observed in the *meso*-**9b**/$AgPF_6$ complex (Figure 9d). The H20–benzene plane (C12 to C17) and H27–benzene plane (C19 to C24) distances are 2.673 and 2.879 Å, respectively. These distances are comparable with typical CH–π distances in aromatic rings.[12] On the other hand, in the *meso*-**9a**/$AgClO_4$ (Figure 9a) and *meso*-**9c**/$AgClO_4$ (Figure 9c) complexes, two aromatic side-arms at the 1- and 10-positions cover the Ag^+, while the third side-arm at the 7-position does not cover. The Ag–ClO_4 bond lengths of the *meso*-**9a**/$AgClO_4$ (Figure 9a) and *meso*-**9c**/$AgClO_4$ are in the range 2.344–2.600 Å. These distances are typical Ag–ClO_4 bond distances.[12] The coordination of ClO_4^- to the Ag^+ bond would prevent the Ag^+–π interaction in the solid state. Interestingly, mean average derivations of Ag^+–N distances in the Ag^+ complexes with **9a**, **9b**, and **9c** are greater than those of tetra-armed cyclens previously reported (Table 1S in the ESI). Interestingly, mean average derivations of Ag^+–N atoms in the Ag^+ complexes with **9a**, **9b**, and **9c** are greater than those of tetra-armed cyclens previously reported (Table 1S in the ESI). The deviations mean that the cyclen rings distorted in the Ag^+ complexes with triple-armed cyclens. The smaller log K values in the triple-armed cyclens (log K = 5.6–6.5) than those of tetra-armed cyclens (log K = 6.8)[2c, 2e] would be due to the ring distortions.

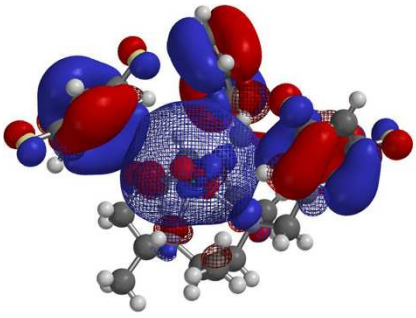

Figure 10. The LUMO and HOMOs calculated by the DFT method [B3LYP/3-21G(*)] using the X-ray structures of the *meso*-**9c**/Ag^+ complex (Isosurface value is 0.02 au). LUMO (mesh) and HOMO[–4], HOMO[–5], and HOMO[–7] (solid).

To visualize the Ag^+–π interactions, the LUMO and HOMOs were calculated by the DFT method [B3LYP/3-21G(*)] using the X-ray structures of the *meso*-**9c**/$AgPF_6$ complex. As shown in Figure 10, LUMO of Ag^+ has contact with HOMOs of the aromatic side-arms. However, in this case, significant distortion of the LUMO like tetra-armed cyclen/Ag^+ complexes was not observed. This result indicates that the Ag^+–π interactions in the triple-armed cyclen/Ag^+ complex would not be so strong interactions.

Conclusions

In the introduction part, we described three questions for the triple-armed cyclens. Now we can answer the questions as follows. (i) The ^{1}H NMR and UV-vis titration experiments showed that the triple-armed cyclens behave like an insectivorous plant (Venus flytrap), thus the three aromatic side-arms cover the Ag+ incorporated in the cyclen cavities. X-ray structures exhibited that Ag^+–π interactions as well as C-H–π interactions are crucial for triple-armed cyclens to work as argentivorous molecules. (ii) When two kinds of aromatic rings are introduced as side-arms, the chemical shift of the protons at the 2'- and 6'-positions in the side-arms changed systematically depending on the next neighbor benzenes. (iii) The inversion barrier between Δ and Λ forms of *meso*-**9b** was estimated to be 11 kcal/mol by VT ^{1}H NMR studies. Synthesis, complexing property towards Ag^+, and chiral enhancement by chiral argentivorous molecules are now in progress in our laboratory.

Dalton

RSCPublishing

ARTICLE

Table 2. Crystal data of *meso*-**6**, *meso*-**9a**/$AgClO_4$, *meso*-**9b**/$AgPF_6$, and *meso*-**9c**/$AgClO_4$.

Compound	*meso*-**6**	*meso*-**9a**/$AgClO_4$	*meso*-**9b**/$AgPF_6$	*meso*-**9c**/$AgClO_4$
Formula	$C_{10}H_{20}N_4O_2$	$C_{31}H_{44}AgClN_4O_5$	$C_{32}H_{42}AgF_{10}N_4OP$	$C_{32}H_{37}AgCl_4N_4O_4$
M	228.30	696.02	827.54	905.33
T/K	273	173	90	120
Crystal system	Monoclinic	Monoclinic	Monoclinic	Monoclinic
Space group	P2(1)/c	P2(1)	P2(1)/c	P2(1)/c
a/Å	9.6821(6)	8.8291(4)	10.6718(6)	19.0094(10)
b/Å	16.7879(10)	20.5803(10)	15.1390(9)	9.2229(5)
c/Å	14.9185(9)	17.8396(8)	23.2571(11)	22.7450(12)
β/ °	102.0980(10)	94.1870(10)	116.497(2)	113.5130(10)
U/Å^3	2371.0(2)	3232.9(3)	3362.7(3)	3656.6(3)
Z	8	4	4	4
D_c/g cm^{-3}	1.279	1.430	1.635	1.645
μ/mm^{-1}	0.091	0.750	0.736	0.917
Data/restraints/parameters	6611/0/325	12943/107/769	7688/0/453	9097/0/466
No. reflns used [>2σ(*I*)]	6611 [R(int)=0.0354]	12943 [R(int) = 0.0168]	7688 [R(int) = 0.0234]	9097 [R(int) = 0.0268]
R_1 ,wR_2 [I>2σ(*I*)]	0.0499, 0.1162	0.0322, 0.0874	0.0314, 0.0822	0.0329, 0.0857
R_1 ,wR_2 [all data]	0.0754, 0.1282	0.0347, 0.0941	0.0341, 0.0857	0.0403, 0.0965
Absolute structure parameter		-0.033(16)		
GOF	1.030	1.076	1.051	1.130

EXPERIMENTAL SECTION

General information

Melting points were obtained with a Mel-Temp capillary apparatus and were not corrected. FAB mass spectra were obtained using a JEOL 600 H mass spectrometer. ^{1}H NMR spectra were measured in $CDCl_3$, CD_2Cl_2, or a mixture of CD_2Cl_2 and CD_3OD on a JEOL ECP400 (400 MHz) spectrometer. UV-vis spectra were recorded on a JASCO V-550 spectrometer. The elemental analysis was carried out on a Yanako MT-6 CHN Micro Corder. All reagents were standard analytical grade and were without further purification. Optical rotations were measured on a digital polarimeter JASCO DIP-360.

Ethyl (S)-2-[[(4-Methylphenyl)sulfonyl]oxy]propionate (*S*)-2. (*S*)-**2** was prepared according to the literature.[5] Yield 97 %. Pare yellow oil. $[\alpha]^D$ = –30.5 (*c* = 2.69, $CHCl_3$). ^{1}H NMR ($CDCl_3$): δ 7.82 (d, *J* = 8.2 Hz, 2H), 7.35 (d, *J* = 8.2 Hz, 2H), 4.93 (q, *J* = 7.1 Hz, 1H), 4.12 (dq, J_1 = 7.1 Hz, J_2 = 1.1 Hz, 2H), 2.45 (s, 3H), 1.51 (d, *J* = 7.1 Hz, 3H), 1.21 (t, *J* = 7.1 Hz, 3H). FAB-MS (*m/z*) (matrix: Dithiiothreitol (DTT)/α-Thioglycelol (TG) = 1:1): 273 ([M+1]$^+$, 100 %).

Ethyl L-alaninate hydrochloride (*S*)-4. (*S*)-**4** was prepared according to the literature.[6] Yield 99 %. Mp: 77.0–79.0 °C. $[\alpha]^D$ = +3.2 (*c* = 2.41, CH_3OH). ^{1}H NMR($CDCl_3$): δ 8.75 (s, 3H), 4.30-4.20 (m, 3H), 1.73 (d, *J* = 7.1 Hz, 3H), 1.30 (t, *J* = 7.1 Hz, 3H). FAB-MS (*m/z*) (matrix: DTT/TG = 1:2): 154 ([M+1–HCl]$^+$, 100 %).

Diethyl (2*R*,2'*S*)-2,2'-iminodipropanoate *meso*-5. ***Meso*-5** was prepared according to the literature.[7] Yield 45 %. Colorless oil. ^{1}H NMR ($CDCl_3$): δ 4.22–4.11 (m, 4H), 3.38 (q, *J* = 7.0 Hz, 2H), 1.31 (d, *J* = 7.1 Hz, 6H), 1.28 (t, *J* = 7.1 Hz, 6H). FAB-MS (*m/z*) (matrix: DTT:TG = 1:1): 218 ([M+1]$^+$, 100 %).

(3*R*,5*S*)-3,5-Dimethyl-1,4,7,10-tetraazacyclododecane-2,6-dione *meso*-6. ***Meso*-5** (2.19 g, 10.1 mmol) was dissolved in absolute CH_3OH (250 mL) and then added to a solution of diethylenetriamine (1.05 g, 10.2 mmol) in 250 mL absolute MeOH. The reaction mixture was stirred at 70 °C in argon atmosphere for 7 days, then the solvent was removed under reduced pressure. The *meso*-**6** was afforded as white powder by recrystallization from a mixture of acetonitrile and methanol. Yield 19 %. White solid. Mp: 191–194 °C. ^{1}H NMR ($CDCl_3$): δ 3.55–3.47 (m, 2H), 3.20 (q, *J* = 7.0 Hz, 2H), 3.07–3.00 (m, 2H), 2.95–2.89 (m, 2H), 2.67–2.61 (m, 2H), 1.37 (d, *J* = 7.0 Hz, 6H). FAB-MS (*m/z*) (matrix: DTT:TG = 1:2): 229 ([M+1]$^+$, 100 %). Anal. calcd. for $C_{10}H_{20}N_4O_2$+1/10H_2O: C, 52.20; H, 8.85; N, 24.35. Found: C, C, 52.20; H, 8.85; N, 24.35.

(3*R*,5*S*)-10-Benzyl-3,5-dimethyl-1,4,7,10-tetraazacyclododecane-2,6-dione *meso*-7a. After a mixture of *meso*-**6** (684 mg, 3.00 mmol) and benzaldehydes (1.13 g, 10.6 mmol), in 1,2-dichloroethane was stirred for 24 h at 1 MPa (Argon atmosphere), $NaBH(OAc)_3$ (1.91 g, 9.00 mmol) was added and stirred for 24 h at atmospheric pressure (Argon atmosphere). To the reaction mixture, saturated aqueous

$NaHCO_3$ was added, and the organic layer was separated. The aqueous layer was extracted with $CHCl_3$ (50 mL x 3). The combined organic layer was washed with water, dried over Na_2SO_4, and concentrated. The residual solid was recrystallized from acetonitrile to give *meso*-**7a** as white solid. Yield 0.763 g (80 %). Mp: 174–177 °C. ^{1}H NMR ($CDCl_3$): δ 7.39–7.23 (m, 5H), 3.70 (s, 2H), 3.50–3.45 (m, 2H), 3.22 (q, J = 7.0 Hz, 2H), 3.04–3.97 (m, 2H), 2.62 (t, J = 5.7 Hz, 4H), 1.37 (d, J = 7.0 Hz, 6H). FAB-MS (m/z) (matrix: DTT:TG = 1:2): 319 ([M+1]$^+$, 100 %). Anal. Calcd. for $C_{17}H_{26}N_4O_2$: C, 64.12; H, 8.23; N, 17.60. Found: C, 64.36; H, 8.27; N, 17.84.

(3*R*,5*S*)-10-(3,5-Difluorobenzyl)-3,5-dimethyl-1,4,7,10-tetraazacyclododecane-2,6-dione *meso*-**7b.** *Meso*-**7b** was prepared in a similar manner with the synthetic procedure of *meso*-**7a**. Yield 53 %. White solid. Mp: 198–201 °C. ^{1}H NMR ($CDCl_3$): δ 6.98–6.88 (dd, J = 8.3 Hz, 2H), 6.77–6.73 (m, 1H), 3.68 (s, 1H), 3.53–3.45 (m, 2H), 3.25–3.20 (q, J = 7.1 Hz 2H), 3.13–3.06 (m, 2H), 2.67–2.55 (m, 4H), 1.38 (d, J = 7.1 Hz, 6H). FAB-MS (*m/z*) (matrix: DTT:TG = 1:2): 355 ([M+1]$^+$, 100 %). Anal. Calcd. for $C_{17}H_{24}N_4F_2O_2$: C, 57.61; H, 6.83; N, 15.81. Found: C, 57.70; H, 6.71; N, 15.49.

(6*R*,8*S*)-1-Benzyl-6,8-dimethyl-1,4,7,10-tetraazacyclododecane *meso*-8a. A mixture of *meso*-**7a** (0.637 g, 2.00 mmol) and DIBAL-H (10 mL, 1 M solution in THF) was stirred at 0 °C in argon atmosphere for 1 day. After NaF (3.35 g, 80.0 mmol) in water (1 mL) and benzene (60 mL) was added at 0 °C, the mixture was stirred for 5 h. The reaction mixture was filtered, and the filtrate was concentrated in reduced pressure. Crude *meso*-**8a** was used without further purification. Yield 0.413 g (71%). Mp: 89–93 °C. ^{1}H NMR ($CDCl_3$): δ 7.35–7.20 (m, 5H), 3.62 (s, 2H), 2.94 (br-s, 2H), 2.70–2.47 (m, 10H), 2.38–2.27 (m, 2H), 1.11 (d, J = 7.0 Hz, 6H). FAB-MS (*m/z*) (matrix: DTT:TG = 1:2): 291 ([M+1]$^+$, 100%).

(6*R*,8*S*)-1-(3,5-Difluorobenzyl)-6,8-dimethyl-1,4,7,10-tetraazacyclododecane *meso*-8b. *Meso*-**8b** was prepared in a similar manner with the synthetic procedure of *meso*-**8a** using *meso*-**7b.** Yield 0.306 g (94%). Mp: 83–86 °C. ^{1}H NMR ($CDCl_3$) δ 6.88 (d, J = 8.6Hz, 2H), 6.67 (t, J = 8.6 Hz, 1H), 3.60 (s, 2H), 2.98–2.90 (m, 2H), 2.71–2.56 (m, 8H), 2.55–2.47 (m, 2H), 2.40–2.33 (dd, J_1 = 5.6Hz, J_2 = 6.5, 2H), 1.12 (d, J = 6.5Hz, 6H). FAB-MS (*m/z*) (matrix: DTT:TG = 1:1): 327 ([M+1]$^+$, 100%).

(3*R*,5*S*)-1,7,10-Tribenzyl-3,5-dimethyl-1,4,7,10-tetraazacyclododecane *meso*-9a. After a mixture of *meso*-**8a** (294 mg, 1.01 mmol), benzaldehydes (633 mg, 5.96 mmol), and $NaBH(OAc)_3$ (1.27 g, 5.99 mmol) in 1,2-dichloroethane (10 mL) was stirred for 5 days at rt under Argon atmosphere (atmospheric pressure), saturated aqueous $NaHCO_3$ was added. The organic layer was separated, and the aqueous layer was extracted with $CHCl_3$ (50 mL x 3). The combined organic layer was washed with water, dried over Na_2SO_4, and concentrated. The residual oil was separated and purified by column chromatography on silica-gel ($CHCl_3$: MeOH: NH_3 aq = 5/1/0.06) to give *meso*-**9a** as a pale-yellow oil. Yield 0.142 g (30 %). Pale-yellow oil. ^{1}H NMR (CD_2Cl_2): δ 7.37–7.29 (m, 10H), 7.26–7.19 (m, 5H), 3.82 (d, J = 14.0 Hz, 2H), 3.50 (s, 2H), 3.41 (d, J = 14.0 Hz, 2H), 2.93–2.88 (br, 2H), 2.74–2.60 (m, 4H), 2.49–2.39 (m, 6H), 2.28 (d, J = 14.0 Hz, 2H), 0.95 (d, J = 6.5 Hz, 6H). Anal. Calcd. for $C_{31}H_{42}N_4$+0.25CH_3OH: C, 78.41; H, 9.05; N, 11.70. Found: C, 78.71; H, 8.86; N, 11.33. FAB-MS (*m/z*) (matrix: DTT:TG = 1:1): 471 ([M+1]$^+$, 100%).

(3*R*,5*S*)-10-Benzyl-3,5-dimethyl-1,7-bis[($^2H_5$)phenyl($^2H_1$)methyl]-1,4,7,10-tetraazacyclododecane *meso*-9b. *Meso*-**9b** was prepared in a similar manner with the synthetic procedure of *meso*-**9a** using *meso*-**8a** and benzaldehyde-d_6. Yield 14 %. Brown oil. ^{1}H NMR (CD_2Cl_2): δ7.34–7.18 (m. 5H), 3.82 (s, 0.7H), 3.54 (s, 3.3H), 2.98–2.85 (m, 2H), 2.81–2.47 (m, 8H), 2.46–2.31 (m, 4H), 1.11 (d, J = 6.2 Hz, 6H). MS (*m/z*) (matrix: DTT:TG = 1:1): 483 ([M+1]$^+$, 100%). Anal. Calcd. for $C_{31}H_{29}D_{12}N_4$+H_2O: C, 74.50; H, 6.25; D, 4.84; N, 11.21. Thermal conductivity of hydrogen is almost same with that of deuterium. Apparent H% is calculated as following equation; $H_{apparent}$ % = H_{calcd} % + D_{calcd} %/2 = 6.25% + (4.84/2)% = 8.67 %, where H_{calcd} % and D_{calcd} % are calculated H %, and calculated D %, respectively. Therefore, C, 74.50; H, 8.67; N, 11.21. Found: C, 74.49; H, 8.64; N, 10.88.

(3*R*,5*S*)-10-Benzyl-1,7-bis(3,5-difluorobenzyl)-3,5-dimethyl-1,4,7,10-tetraazacyclododecane *meso*-9c. *Meso*-**9c** was prepared in a similar manner with the synthetic procedure of *meso*-**9a** using *meso*-**8a** and 3,5-difluorobenzaldehyde. Yield 21%. Pale yellow solid. Mp: 90.0–91.5 °C. ^{1}H NMR (CD_2Cl_2): δ 7.35–7.26 (m, 2H), 7.24–7.14 (m, 3H), 6.92 (d, J = 8.7 Hz, 5H), 6.71 (t, J = 8.7 Hz, 2H), 3.80 (d, J = 15.0 Hz, 2H), 3.54 (d, J = 15.0 Hz, 2H), 3.48 (s, 2H), 2.86 (br-s, 2H), 2.77–2.67 (m, 2H), 2.61–2.47 (m, 6H), 2..47–2.33 (m, 4H), 0.96 (br-s, , 6H). MS (*m/z*) (matrix: DTT:TG = 1:1): 543 ([M+1]$^+$, 100%). Anal. Calcd. for $C_{31}H_{38}F_4N_4$+H_2O: C, 68.61; H, 7.06; N, 10.32. Found: C, 68.70; H, 7.07; N, 10.22.

(3*R*,5*S*)-1,7,10-Tris(3,5-difluorobenzyl)-3,5-dimethyl-1,4,7,10-tetraazacyclododecane *meso*-9d. *Meso*-**9d** was prepared in a similar manner with the synthetic procedure of *meso*-**9a** using *meso*-**8b** and 3,5-difluorobenzaldehyde. Yield 44%. Pale yellow solid. Mp: 83.0–86.0 °C. ^{1}H NMR (CD_2Cl_2): δ 6.93 (d, J = 9.1 Hz, 4H), 6.84 (d, J = 9.1 Hz, 2H), 6.72 (t, J = 9.1 Hz, 2H), 6.67 (t, J = 9.1 Hz, 1H), 3.85 (J = 15.3 Hz, 2H), 3.62 (J = 15.3 Hz, 2H), 3.48 (s, 2H), 3.66 (s, 1H), 2.95–2.83 (m, 2H), 2.82–2.69 (m, 4H), 2.68–2.56 (m, 4H), 2.56–2.38 (m, 4H), 1.18–0.99 (br-s, 6H). MS (*m/z*) (matrix: DTT:TG = 1:1): 579 ([M+1]$^+$, 100%). Anal. Calcd. for $C_{31}H_{36}F_6N_4$+1/2H_2O: C, 63.36; H, 6.35; N, 9.53. Found: C, 63.13; H, 6.15; N, 9.16.

Preparation of Silver Ion Complexes. The ligand (0.0151 mmol) in chloroform or dichloromethane (1 mL) was added to the corresponding metal salt ($AgPF_6$ or $AgClO_4$) (0.0153 mmol) in methanol (1 mL). Crystals were obtained quantitatively on evaporation of the solvent.

meso-**9a**/$AgClO_4$. Mp: 112–115 °C (Dec.). Anal. Calcd. for $C_{31}H_{42}AgClN_4O_4$+0.25H_2O: C, 54.55; H, 6.28; N,8.21. Found: C, 54.50; H, 6.25; N, 8.20.

meso-**9b**/$AgPF_6$. Mp: 130–133 °C (Dec.). Anal. Calcd. for $C_{31}H_{38}F_{10}N_4AgP$+CH_3OH: C, 46.45; H, 5.12; N, 6.77 Found: C, 46.79; H, 5.06; N, 6.42.

meso-**9c**/$AgClO_4$. Mp: 143–145 °C (Dec.). Anal. Calcd. for $C_{31}H_{36}AgClF_6N_4O_4$+0.1$CHCl_3$: C, 46.82; H, 4.56; N, 7.02. Found: C, 46.97; H, 4.88; N, 6.85.

^{1}H NMR titration experiments. ^{1}H NMR titration experiments were carried out at 298 K by the addition of 0.2–2.0 equivalents of $AgPF_6$ (1 mmol/μL) in CD_3OD to ligands (5 x 10^{-3} mmol/0.65 mL in CD_2Cl_2).

UV-vis titration experiments. UV-vis titration experiments were carried by addition of 0.1–2.0 equivalents of $AgPF_6$ in CH_3CN (3.0 x 10^{-2} M) to ligands in CH_3CN (1.0 x 10^{-4} M, 3 mL) at 298 K.

X-ray crystallography. Crystals of *meso*-**6**, *meso*-**9a**/$AgClO_4$, *meso*-**9b**/$AgPF_6$, and *meso*-**9c**/$AgClO_4$ were mounted on top of a glass fiber, and data collections were performed using a Bruker SMART CCD area diffractometer at 90–273 K. Data were corrected for Lorentz and polarization effects, and absorption corrections were applied using the SADABS[13] program. Structures were solved by a direct method and subsequent difference-Fourier syntheses using the program SHELEX.[14] All non-hydrogen atoms were refined anisotropically and hydrogen atoms were placed at calculated positions and then refined using $U_{iso}(H) = 1.2U_{eq}(C)$. The crystallographic refinement parameters of the complexes are summarized in Table 2.

Acknowledgements

The authors thank Professor Masatoshi Hasegawa for the TG DTA measurements. This research was supported by Grants-in-Aid 08026969, 11011761 and 26410100, a High-Tech Research Center project (2005–2009), and the Supported Program for Strategic Research Foundation at Private Universities (2012–2016) from the Ministry of Education, Culture, Sports, Science and Technology of Japan for Y.H

Notes and references

[a] Department of Chemistry, Faculty of Science, Toho University, 2-2-1 Miyama, Funabashi, Chiba 274-8510, Japan
[b] Research Center for Materials with Integrated Properties, Toho University, 2-2-1 Miyama, Funabashi, Chiba 274-8510, Japan
[c] Education Center, Faculty of Engineering, Chiba Institute of Technology, 2-1-1 Shibazono, Narashino, Chiba 275-0023, Japan

Electronic Supplementary Information (ESI) available: Spectral data for the synthesized compounds and (PDF). Crystallographic data for *meso*-**6**, *meso*-**9a**/$AgClO_4$, *meso*-**9c**/$AgPF_6$, and *meso*-**9d**/$AgClO_4$ (CIF). See DOI: 10.1039/b000000x/

(1) (a) S. Shinoda, *Chem. Soc. Rev.*, 2013**, 42**, 1825–1835; (b) C. Platas-Iglesias, *Eur. J. Inorg. Chem.*, 2012**, 2012**, 2023–2033; (c) A. Rodríguez-Rodríguez, D. Esteban-Gómez, A. de Blas, T. Rodríguez-Blas, M. Fekete, M. Botta, R. Tripier, C. Platas-Iglesias, *Inorg. Chem.*, 2012, **51**, 2509–2521; (d) B. P. Burke, G. S. Clemente, S. J. Archibald, *J. Labelled Compd. Radiopharm.*, 2014, **57**, 239–243; (e) T. Y. Lee, J. Suh, *Pure Appl. Chem.*, 2009, **81**, 255–262.

(2) (a) Y. Habata, M. Ikeda, A. K. Sah, K. Noto, S. Kuwahara, *Inorg. Chem.*, 2013, **52**, 11697–11699; (b) Y. Habata, Y. Okeda, M. Ikeda, S. Kuwahara, *Org. & Biomol. Chem.*, 2013, **11**, 4265–4270; (c) Y. Habata, Y. Oyama, M. Ikeda, S. Kuwahara, *Dalton Trans.*, 2013, **42**, 8212–8217; (d) Y. Habata, A. Taniguchi, M. Ikeda, T. Hiraoka, N. Matsuyama, S. Otsuka, S. Kuwahara, *Inorg. Chem.*, 2013, **52**, 2542–2549; (e) Y. Habata, M. Ikeda, S. Yamada, H. Takahashi, S. Ueno, T. Suzuki, S. Kuwahara, *Org. Lett.*, 2012, **14**, 4576–4579.

(3) (a) G. A. Bowmaker, Effendy, M. Nitiatmodjo, B. W. Skelton and A. H. White, *Inorganica Chimica Acta*, 2005, **358**, 4327-4341; (b) M. Wen, M. Munakata, Y. Suenaga, T. Kuroda-Sowa, M. Maekawa and I. Kodai, *Polyhedron*, 2004, **23**, 2117-2123.

(4) "Argentivorous" is different from "argentophilic". "Argentophilic" is used in the sense of Ag^+–Ag^+ interactions. For example, (a) E. C. Constable, C. E. Housecroft, P. Kopecky, M. Neuburger and J. A. Zampese, *Inorg. Chem. Commun.*, 2013, **27**, 159-162; (b) G.-G. Luo, D.-L. Wu, L. Liu, S.-H. Wu, D.-X. Li, Z.-J. Xiao and J.-C. Dai, *J. Mol. Struct.*, 2012, **1014**, 92-96; (c) R. Santra, M. Garai, D. Mondal and K. Biradha, *Chemistry*, 2013, **19**, 489-493; (d) G. A. Senchyk, V. O. Bukhan'ko, A. B. Lysenko, H. Krautscheid, E. B. Rusanov, A. N. Chernega, M. Karbowiak and K. V. Domasevitch, *Inorg. Chem.*, 2012, **51**, 8025-8033; (e) A. Stephenson and M. D. Ward, *Chem. Commun.*, 2012, **48**, 3605-3607; (f) J. Xu, S. Gao, S. W. Ng and E. R. T. Tiekink, *Acta Crystallogr Sect E Struct Rep Online*, 2012, **68**, m639-640; (g) J. Xu, S. Gao, S. W. Ng and E. R. T. Tiekink, *Acta Crystallogr., Sect. E: Struct. Rep. Online*, 2012, **E68**, m639-m640; (h) G. Yang, P. Baran, A. R. Martinez and R. G. Raptis, *Cryst. Growth Des.*, 2013, **13**, 264-269.

(5) R. W. Brown, *J. Agric. Food Chem.*, 1990, **38**, 269–273.

(6) T. Jakusch, A. Dornyei, I. Correia, L. M. Rodrigues, G. K. Toth, T. Kiss, J. C. Pessoa, S. Marcao, *Eur. J. Inorg. Chem.*, 2003, 2113–2122.

(7) S. S. Insaf, D. T. Witiak, *Tetrahedron*, 2000, **56**, 2359–2367.

(8) Spartan'10, Wavefunction, Inc., Irvine, CA; (b) W. J. Hehre, J. Yu, P. E. Klunzinger and L. Lou, A Brief Guide to Molecular Mechanics and Quantum Chemistry Calculations, Wavefunction, Irvine, CA, 1998, p. 159.

(9) H. Shanan-Atidi, K. H. Bar-Eli, *J. Phys. Chem.*, 1970, **74**, 961–963.

(10)P. Gans, A. Sabatini, A. Vacca, *Talanta*, 1996, **43**, 1739–1753.

(11)(a) M. Nishio, Y. Umezawa, M. Hirota, Y. Takeuchi, *Tetrahedron*, 1995, 51, 8665–8701; (b) M. Abe, M. Eto, K. Yamaguchi, M. Yamasaki, J. Misaka, Y. Yoshitake, M. Otsuka, K. Harano, *Tetrahedron*, 2012, **68**, 3566–3576.

(12)(a) D.-Z. Wang, *J. Mol. Struct.*, 2009, **929**, 128–133; (b) J. Y. Liu, Z. Y. Liu, J. J. Zhang, Y. Y. Wang, P. Yang, Y. Wang, B. Ding, B.X. J. Zhao, *CrystEngComm*, 2013, **15**, 6413–6423; (c) F. Jin, X.–F. Yang, S.-L. Li, Z. Zheng, Z.-P. Yu, L. Kong, F.-Y. Hao, J.-X. Yang, J.-Y. Wu, Y.-P. Tian, H.-P. Zhou, *CrystEngComm*, 2012, **14**, 8409–8417; (d) C. V. K. Sharma, R. D. Rogers, *Cryst. Eng.*, 1998, **1**, 19–38; (e) S.-M. Fang, S.-T. Ma, L.-Q. Guo, Q. Zhang, M. Hu, L.-M. Zhou, L.-J. Gao, C.-S. Liu, *Inorg. Chem. Commun.*, 2010, **13**, 139–144; (f) G.-l. Zheng, H.-J. Zhang, S.-Y. Song, Y.-Y. Li, H.-D. Guo, *Eur. J. Inorg. Chem.*, 2008, 1756–1759; (g) H. Wu, X.-W. Dong, H.-Y. Liu, J.-F. Ma, Y.-Y. Liu,; Y.-Y. Liu, J. Yang, *Inorg. Chim. Acta*, 2011, **373**, 19–26; (h) R. H. Laye, *Inorg. Chim. Acta*, 2007, **360**, 439–447; (i) Z.-P. Deng, L.-N. Zhu, S. Gao, L.-H. Huo, S. W. Ng, *Cryst.*

Growth Des., 2008, **8**, 3277–3284; (j) B. N.Ahamed, M. Arunachalam, P. Ghosh, *Inorg. Chem.*, 2011, **50**, 4772–4780; (k) T. Mochida, K. Okazawa, R. Horikoshi, *Dalton Trans.*, 2006, 693–704; (l) Y.-B. Xie, C. Zhang, J.-R. Li, X.-H. Bu, *Dalton Trans.*, 2004, 562–569; (m) L. Wang, T. Tao, S.-J. Fu, C. Wang, W. Huang, X.-Z. You, *CrystEngComm*, 2011, **13**, 747–749; (n) G. A. Bowmaker, Effendy, M. Nitiatmodjo, B. W. Skelton, A. H. White, *Inorg. Chim. Acta*, 2005, **358**, 4327–4341; (o) Q. Sun, M. Wei, Y. Bai, C. He, Q. Meng, C. Duan, *Dalton Trans.*, 2007, 4089–4094; (p) G. Yang, S.-L. Zheng, X.-M. Chen, H. K. Lee, Z.-Y. Zhou, T. C. W. Mak, *Inorg. Chim. Acta*, 2000, **303**, 86–93; (q) N. J. Williams, W. Gan, J. H. Reibenspies, R. D. Hancock, *Inorg. Chem.*, 2009, **48**, 1407–1415.

(13)SADABS, version 2.03; G. M. Sheldrick, Program for adsorption correction of area detector frames, Bruker AXS, Inc., Madison, WI, 1996.

(14)SHELXTLTM, version 5.1; Bruker AXS, Inc., Madison, WI, 1997.

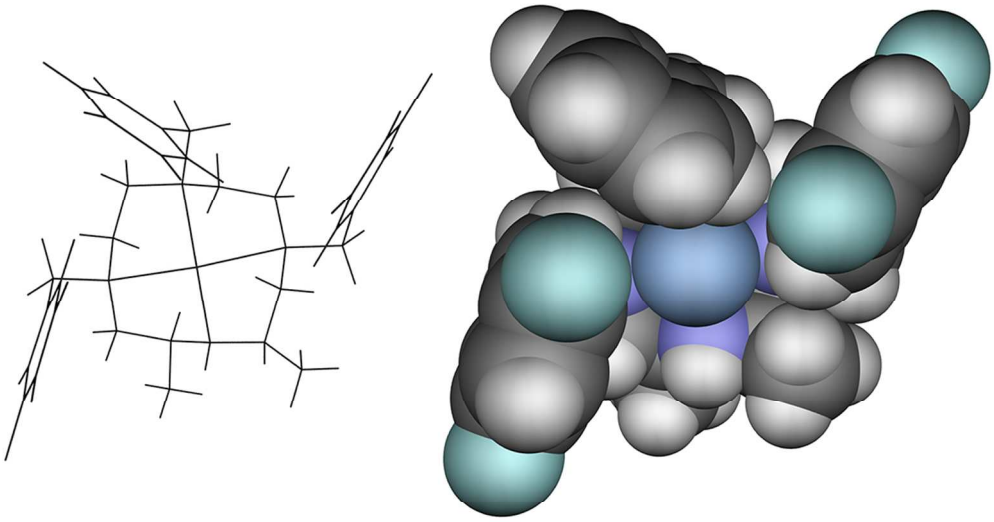

Ag^{+}–π and C-H–π interactions

99x60mm (300 x 300 DPI)